HHS Public Access

Author manuscript

J Immunol. Author manuscript; available in PMC 2017 April 01.

Published in final edited form as:

J Immunol. 2016 April 1; 196(7): 3054–3063. doi:10.4049/jimmunol.1501797.

Shortened intervals during heterologous boosting preserve memory CD8 T cell function but compromise longevity

Emily A. Thompson[*], **Lalit K. Beura**[*], **Christine E. Nelson**[*], **Kristin G. Anderson**[†], and **Vaiva Vezys**[*]

[*]Department of Microbiology and Immunology, Center for Immunology, University of Minnesota, Minneapolis, MN, 55455

[†]Department of Medicine, Division of Oncology, University of Washington, Fred Hutchinson Cancer Research Center, Seattle, WA, 98109

Abstract

Developing vaccine strategies to generate high numbers of Ag-specific CD8 T cells may be necessary for protection against recalcitrant pathogens. Heterologous prime-boost-boost (HPBB) immunization has been shown to result in large quantities of functional memory CD8 T cells with protective capacities and long-term stability. Completing the serial immunization steps for HPBB can be lengthy, leaving the host vulnerable for an extensive period of time during the vaccination process. We show here that shortening the intervals between boosting events to 2 weeks results in high numbers of functional and protective Ag-specific CD8 T cells. This protection is comparable to that achieved with long-term boosting intervals. Short-boosted Ag-specific CD8 T cells display a canonical memory T cell signature associated with long-lived memory, have identical proliferative potential to long-boosted T cells and both populations robustly respond to antigenic re-exposure. Despite this, short-boosted Ag-specific CD8 T cells continue to contract gradually over time, which correlates to metabolic differences between short- and long-boosted CD8 T cells at early memory timepoints. Our studies indicate that shortening the interval between boosts can yield abundant, functional Ag-specific CD8 T cells, which are poised for immediate protection; however, this is at the expense of forming stable long-term memory.

Introduction

Vaccine strategies that are able to generate high frequencies of memory CD8 T cells may be essential to prevent or limit infections by pathogens such as HIV, *Mycobacterium tuberculosis*, *Plasmodium falciparum*, hepatitis C virus and influenza viruses, where humoral immunity may not be sufficient for protection (1–6). Memory CD8 T cells are poised to perform a diverse set of effector functions upon Ag re-encounter. Central memory T cells (T_{CM}) proliferate rapidly after recall, while effector memory cells (T_{EM}) are capable of rapid degranulation and cytokine release (7–9). Tissue resident memory (T_{RM}) CD8 T cells are positioned at the frontlines and contain invading pathogens by inducing an anti-

Corresponding author address: Vaiva Vezys, 2-180 WMBB, 2101 6th St SE, Minneapolis, MN 55455, vvezys@umn.edu, phone 612-625-4650, fax 612-625-2199.

viral state to prevent systemic infection (10, 11). These diverse functional properties of memory CD8 T cells make them an important component of the immune response and a critical cell type elicited by certain vaccines.

Heterologous prime-boost-boost (HPBB) strategies have been shown to generate large quantities of Ag-specific CD8 T cells that rapidly develop into memory CD8 T cells, which remain stable and contract very little over time, accelerating protection upon pathogen re-encounter (12, 13). This is a multi-step immunization scheme, where the host is exposed to different vaccine vectors containing a common protein or epitope to stimulate CD8 T cells of interest (14, 15). While this method generates large numbers of long lasting memory CD8 T cells, the time intervals between each boost are at least 28 days long and can be as long as six months. This may not be ideal in situations where protection needs to be achieved quickly, such as during an outbreak. We have learned from current licensed Ab based vaccine regimens that lengthy intervals between boosts can contribute to poor vaccine compliance (16, 17). In fact, nearly 28% of children surveyed did not comply with their vaccination schedule (18). Other studies showed that vaccine non-compliance can be as low as 30% in older children and adult populations (19). This lack of compliance and failure to complete vaccination regimens are acknowledged to contribute to increased infection and disease incidence for many pathogens, which can be controlled by efficient vaccination. It is therefore of interest to develop vaccine strategies that decrease total immunization time, yet generate protective immunity.

We sought to identify methods to more rapidly generate protective memory CD8 T cells. This has been explored in a system where primary FluMist responses were boosted 7 days later with recombinant *Listeria monocytogenes* (LM), yielding protection against lethal influenza challenge (20). Wong et al., have demonstrated protection against a bacterial challenge by boosting primary LM responses 7 days later with a heterologous vector (21). Interestingly, rapid boosting has also shown to improve survival from tumor challenge using a vesicular stomatitis virus (VSV)-human dopachrome tautomerase (hDCT) prime followed by an adenovirus-hDCT boost within as little as 4 days (22). Additional studies show that CD8 T cell immunization in settings of low inflammation results in rapid development of memory phenotype CD8 T cells, which respond within days to boosting and protect against microbial challenge (23, 24).

While the above studies demonstrate that shortening boosting intervals can generate protective CD8 T cells, direct comparisons between short and long-term boosting efficacy remain to be extensively explored. It is unknown how the longevity of memory CD8 T cells is affected when using short-boosting regimens. Therefore, in this study we shortened boosting intervals between three sequential, non-cross-reactive vectors to examine how this impacts CD8 T cell phenotype, effector function, quantity, location and longevity. We found that short HPBB results in large numbers of Ag-specific CD8 T cells that are as protective and functional as T cells generated using longer intervals between boosts. Interestingly, while CD8 T cells generated using shortened boost intervals express canonical memory markers, they fail to survive long-term and continue to gradually contract over time. This correlates with differences in metabolic activity at early memory timepoints following the tertiary boost. These results reveal that short-boosting intervals can generate effector Ag-

specific CD8 T cells that are comparable in measures of standard function and protection against challenge to long-term boosted CD8 T cells. However, brief boosting intervals come at the cost of compromising memory T cell longevity. This suggests that while short-boosting is useful for establishing protection rapidly, additional measures, such as future boosts, may need to be implemented to prevent contraction of the short-boosted CD8 T cell memory population.

Materials and Methods

Mice and Infections

C57BL/6J and *Ptprc$_a$ PepC$_b$*/BoyJ (CD45.1) mice were purchased from The Jackson Laboratory (Bar Harbor, ME) or The National Cancer Institute (Frederick, MD). To generate short-boosted mice, animals were primed with 1×10^6 PFU VSV-OVA i.v. (1°), rested for 14 days, boosted with 1×10^4 CFU LM-OVA i.v. (2°), rested for 14 days, then given an additional boost with 2×10^6 PFU vaccinia virus (VV)-OVA i.v. (3°) (25–27). Long-term boosted mice were generated with this same regimen, but with at least 28 days rest between each boost. All mice were used in accordance with the National Institutes of Health and the University of Minnesota Institutional Animal Care and Use Committee guidelines.

Intravascular staining, Isolation of lymphocytes and Flow cytometry

To discriminate between CD8 T cells in tissue parenchyma versus tissue vasculature, i.v. injected Ab was used as previously described (28). Briefly, 3μg of anti-CD8α Ab (53-6.7, Biolegend, San Diego, CA) was injected i.v. and allowed to circulate for three minutes prior to mouse sacrifice.

Organs were harvested and digested as previously described (29). For isolation of small intestinal intraepithelial lymphocytes (IEL), Peyer's patches were removed, the small intestine was cut longitudinally and then laterally into small pieces. Pieces were incubated for 30 minutes with stirring at 37°C with 0.154mg/mL dithioerythritol (Sigma-Aldrich, St. Louis, MO) in 10% HBSS/HEPES. Female reproductive tract (FRT), lung and salivary gland (SG) tissues were cut into small pieces in RPMI 1640 containing 5% FBS, 2 mM $MgCl_2$, 2 mM $CaCl_2$ and 0.5mg/mL type IV collagenase for FRT (Sigma-Aldrich, St. Louis, MO) or 100 U/mL type I collagenase for lung and SG (Worthington, Lakewood, NJ) and incubated for 1 hr at 37°C with stirring. After enzymatic digestion, the remaining tissue pieces were mechanically disrupted using a gentleMACs dissociator (Miltenyi Biotec, San Diego, CA). The liver was mechanically dissociated by pushing the tissue through a 70μm-cell strainer. Single cell suspensions of IEL, FRT, lung, liver and SG were further separated using a 44/67% Percoll (GE Healthcare Life Sciences, Pittsburgh, PA) density gradient. Spleen and lymph nodes (LN) were dissociated mechanically. Splenocytes and blood were treated with ACK lysis buffer to lyse red blood cells.

The following antibodies were used for flow cytometry: anti-KLRG1 (2F1), anti-Eomes (Dan11ma), anti-T-bet (4B10), anti-CD44 (IM7), anti-CD122 (TM-b1), anti-CD27 (LG. 7F9), anti-CD69 (H1.2F3) (all from eBioscience, San Diego, CA), anti-CD8α (53-6.7, eBioscience, Biolegend, San Diego, CA), anti-CD103 (M290), anti-CD25 (PC61), anti-

Bcl-2 (Bcl-2/100) and anti-CD127 (SB/199) (BD Biosciences, San Jose, CA). Cell viability was determined using Ghost Dye™ Red 780 (Tonbo Biosciences, San Diego, CA). K^b-SIINFEKL-specific CD8 T cells were identified using H-2K^b tetramers made in house containing the SIINFEKL peptide (New England Peptide, Gardener, MA). The BD Biosciences intracellular kit for cytokine staining and the eBioscience FoxP3 kit for transcription factor staining were used in accordance with manufacturer's directions. Peptide stimulation was performed as previously described (30). Briefly, splenocytes were plated in RPMI 1640 containing 10% FBS, 1× NEAA, 2mM L-glutamine, 1mM sodium pyruvate, 1× penicillin/streptomycin and 0.05mM β-mercaptoethanol and incubated with 1ug/mL SIINFEKL peptide and 1ug/mL GolgiPlug (BD Biosciences, San Jose, CA) for four hours at 37°C. Cells were washed and stained with fixable LIVE/DEAD aqua dead cell stain (Life Technologies, San Diego, CA) before surface and intracellular staining. Samples were acquired on an LSRII flow cytometer (BD Biosciences, San Diego, CA).

Recall and Protection Assays

For transfer and recall experiments, CD8 T cells were enriched from splenocytes of CD45.2 mice at day 30 or ≥95 after 3° using an EasySep CD8+ T cell isolation kit (STEMCELL Technologies, Vancouver, Canada). For early memory transfers, 2.5×10^5 K^b-SIINFEKL-specific CD8 T cells were transferred i.v. to CD45.1 mice. For late memory transfer experiments, cells were flow sorted and either 2×10^3 or 2×10^5 K^b-SIINFEKL-specific CD8 T cells were transferred i.v. to CD45.1 mice. In all cases, recipient mice were infected i.v. with 1×10^6 PFU of VSV-OVA the day after cell transfer.

To determine the ability of T cells to protect upon re-infection, 3° short-boosted and long-boosted mice were generated as described above and sacrificed five days after infection with 2×10^6 PFU VV-OVA i.v. (the 3° boost). Ovaries and spleen were harvested, homogenized and viral loads were analyzed by plaque assays on 143B cells, as previously described (31). Naïve mice were infected with 2×10^6 PFU VV-OVA i.v. as a control.

Metabolic Assays

CD8 T cells were enriched using an EasySep CD8 T cell isolation kit (STEMCELL Technologies, Vancouver, Canada) and K^b-SIINFEKL-specific CD8 T cells were purified from the resulting population using flow cytometric sorting. At day 30, day 51 and day 69 following 3° short- or long-boost, Ag-specific CD8 T cells were plated at 2-8.5 × 10^5 cells/well (cell numbers were kept similar within experiment) in non-buffered, sodium bicarbonate free, RPMI 1640 containing 25mM glucose, 2mM L-glutamine and 1mM sodium pyruvate. For day 69 experiments, cells were pooled from 2 to 9 short-boosted mice or up to 3 long-boosted mice. Oxygen consumption rate (OCR) was evaluated using the Seahorse XF-24 Extracellular Flux Analyzer (Seahorse Bioscience, Billerica, MA). The non-corrected basal OCR was directly measured, followed by the addition of 0.0063mM oligomycin (Sigma-Aldrich, St. Louis, MO) to evaluate ATP production. Non-corrected maximum OCR was examined by addition of 0.015mM fluoro-carbonyl cyanide phenylhydrazone (FCCP) (Sigma-Aldrich, St. Louis, MO) and non-mitochondrial respiration was measured following the addition of 0.019mM rotenone (Sigma-Aldrich, St. Louis, MO). Corrected basal OCR, corrected maximal OCR and spare respiratory capacity

(SCR) were calculated as shown earlier (32). Briefly, to calculate corrected basal OCR and corrected maximum OCR, non-mitochondrial respiration was subtracted from basal and maximum OCR. SRC was determined by subtracting corrected basal OCR from corrected maximum OCR.

Statistical Analysis

An unpaired two-tailed Student's *t*-test was performed when groups were compared using Prism (GraphPad Software Inc.). For all analysis, *p* values of less than 0.05 were considered significant and were indicated by asterisks (*).

Results

Short intervals between heterologous boosts generate large numbers of Ag-specific CD8 T cells

To test the ability of short heterologous prime-boost-boost (HPBB) intervals to generate a high number of Ag-specific CD8 T cells, three replicating vectors encoding OVA were administered to mice 14 days apart (Figure 1A). Mice were sacrificed at days 7 and 14 following 1° (VSV-OVA), 2° (VSV-OVA + LM-OVA), or 3° (VSV-OVA + LM-OVA + VV-OVA) vaccinations and the frequency and numbers of K^b-SIINFEKL-specific CD8 T cells were evaluated in peripheral blood lymphocytes (PBL), spleen and small intestinal intraepithelial lymphocytes (IEL) (Figures 1B-F).

The frequency of K^b-SIINFEKL-specific CD8 T cells in PBL at day 7 increased after each vaccination, on average from 9.5% of total CD8 T cells at 1° to 31% at 2° and 51% after 3° (Figures 1B, D). An increase in Ag-specific CD8 T cell frequency at this timepoint was also noted in spleen throughout the vaccination regimen (Figure 1B). Notably, K^b-SIINFEKL-specific CD8 T cells increased more robustly in PBL then spleen with each boost (Figure 1B). By day 14, a decrease in K^b-SIINFEKL-specific CD8 T cells was observed relative to the percent of cells present at day 7 after 1° or 2° boosting events (Figures 1B-C). Enumeration of total numbers of K^b-SIINFEKL-specific CD8 T cells in the spleen revealed that this shortened boosting strategy induced large numbers of Ag-specific CD8 T cells (Figure 1E). Indeed, nearly 6×10^6 cells were present at day 7 following 3° boost and at day 14 there was no evidence of contraction. Ag-specific CD8 T cells in the IEL also expanded after immunization (Figure 1F). While there was a loss of K^b-SIINFEKL-specific CD8 T cells in this compartment between days 7 and 14 after 3° boosting, heterologous boosting increased the numbers of Ag-specific CD8 T cells approximately 5.5-fold when compared to cell numbers at day 14 after the 1° vaccination step. In conclusion, the immunization regimen with short intervals was able to generate abundant Ag-specific CD8 T cells.

Ag-specific CD8 T cells generated with short HPBB migrate to and populate multiple non-lymphoid tissues

We evaluated whether T cells generated following short-boosting intervals could access non-lymphoid tissues (NLT) and establish broadly distributed memory. At least 95 days after 3° immunization, K^b-SIINFEKL-specific CD8 T cells were enumerated in spleen, inguinal lymph nodes (IgLN), IEL, lung, liver, female reproductive tract (FRT) and salivary

gland (SG) (Figures 2A-B). In these tissues, Ag-specific CD8 T cells were readily detected, indicating efficient seeding of K^b-SIINFEKL-specific CD8 T cells to NLT, as described previously (33). The frequencies of Ag-specific CD8 T cells in most NLT were greater than those in the secondary lymphoid organs: ~40% of CD8 T cells were specific for the OVA vaccine insert. In PBL, ~30% of CD8 T cells were K^b-SIINFEKL-specific CD8 T cells (Figure 2A).

Contact between CD8 T cells and infected targets is essential for efficient pathogen control. Thus, the location of Ag-specific T cells within tissue parenchyma or tissue vasculature was determined by using a previously described i.v. Ab staining technique (Figure 2C) (28). This technique selectively labels cells in the vasculature of a tissue by i.v. injecting fluorochrome-labeled Ab. Cells that are in the tissue parenchyma are not accessed by Ab and will remain unlabeled. At least 95 days after 3° boosting, K^b-SIINFEKL-specific CD8 T cells in the spleen were distributed evenly between white pulp and red pulp at a 1:1 ratio (Figures 2C-D). As expected, the distribution of cells in the IgLN was biased to the i.v. Ab negative compartment and in the PBL was biased to the i.v. Ab positive compartment. Ag-specific CD8 T cells in the lung and liver were predominantly found in the vasculature, while K^b-SIINFEKL-specific CD8 T cells in the FRT were evenly distributed between i.v. Ab positive and i.v. Ab negative fractions (Figures 2C-D). Intravenous Ab negative cells in IgLN had high expression of CD62L while cells in the spleen, IEL, lung, liver, FRT and SG were CD62L low (Supplementary Figure 1A). While most of K^b-SIINFEKL-specific CD8 T cells in secondary lymphoid organs (SLO) were CD103 and CD69 negative, the majority of cells in the IEL and SG were positive for both of these markers. Ag-specific CD8 T cells in the i.v. Ab negative fraction in the FRT displayed bimodal expression of CD69 but were not CD103 positive (Supplementary Figure 1B-C). In summary, CD8 T cells activated after the short-boost immunization scheme penetrated multiple NLTs and exhibit phenotypes consistent with T_{EM} and T_{RM} cells.

Ag-specific CD8 T cells have similar functionality regardless of immunization interval length

We went on to assess the functionality of the CD8 T cells generated after short-boost vaccination compared to cells produced after longer immunization intervals. Granzyme B expression was evaluated at day 5 after 3° immunization and compared between short- and long-boosted T cells. On a per cell basis, granzyme B production was similar in both populations of Ag-specific CD8 T cells indicating equal ability to kill target cells (Figure 3A). At this same time point, the protective capacity of effector CD8 T cells generated by short- and long- boosting was evaluated by quantifying vaccinia virus titers. In spleen, viral titers in long- and short-boosted mice were not detectable, while infected naïve mice, which do not have K^b-SIINFEKL-specific memory CD8 T cells, had a significantly higher viral load (~10^4 PFU) (Figure 3B). In the ovaries, a primary site of vaccinia virus replication, there was a significant decrease in viral titers in both long-boosted mice and short-boosted mice, as compared to titers in naïve, infected animals (Figure 3C).

To evaluate Ag-specific T cell function after the final boost, K^b-SIINFEKL-specific CD8 T cells were examined for cytokine production following SIINFEKL peptide re-stimulation at

day 14 after 3° short and long HPBB. Ag-specific short-boosted CD8 T cells were able to produce interferon-γ (IFNγ) and tumor necrosis factor-α (TNFα) in response to SIINFEKL peptide at a similar capacity as long-boosted T cells (Figure 4A). Importantly, equal numbers of Ag-specific T cells are generated, regardless of boosting history and all of these cells produced IFNγ cytokine (Figures 4A-B).

To investigate if short-boosted T cells are able to proliferate upon recall as well as long-boosted T cells, 32 days after 3°, equal numbers of K^b-SIINFEKL-specific memory CD8 T cells from short- or long-term boosted mice were transferred into naïve CD45.1 recipients, which were then infected with VSV-OVA. Enumeration of donor K^b-SIINFEKL-specific CD8 T cells at day 6 after infection revealed that both populations expanded similarly regardless of previous boosting history, indicating similar proliferative potential between these cells (Figure 4C).

To determine if the proliferative potential of short-boosted T cells was maintained until a late memory time point, we also evaluated the ability of K^b- SIINFEKL-specific CD8 T cells to expand upon recall at least 95 days after 3°. Either 2×10^3 or 2×10^5 K^b-SIINFEKL-specific CD8 T cells from short-boosted or long-boosted mice were transferred to naive CD45.1 recipients and infected 1 day later with VSV-OVA. The two different input numbers of cells were chosen to eliminate the impact of transferring large numbers of cells on individual T cell functions. We tracked donor Ag-specific CD8 T cells in the blood of recipient mice following infection to determine the timing of peak expansion. Whether a low or high number of cells were transferred, short-boosted T cells expanded as well as long-boosted T cells upon recall. The peak of expansion was similar for both populations of transferred cells, although lower cell number inputs resulted in a delayed response (Figure 4D). At all timepoints, there was no significant difference between the short- and long-boosted cell populations. 22 days later, Ag-specific CD8 T cells were enumerated in the spleen (Figure 4E). The number of donor short-boosted and long-boosted K^b-SIINFEKL-specific CD8 T cells in mice receiving low numbers of cells was not statistically different. Similarly, donor short-boosted and long-boosted K^b-SIINFEKL-specific CD8 T cells seeded at high numbers were also not statistically different, but more cells were recovered with high transfer. Taken together, both short and long immunization schema-derived Ag-specific CD8 T cells displayed similar functionality.

Ag-specific CD8 T cells generated through short-boosting display a memory phenotype

HPBB with long-boost intervals results in stable CD8 T cell memory that contracts very little over time (12, 13). It might be expected that shortening the immunization intervals would result in a terminally differentiated population of cells, due to an increased inflammatory environment and more frequent Ag contact. To evaluate whether short-boosted Ag-specific CD8 T cells could differentiate into classical memory T cells, K^b-SIINFEKL tetramer+ cells were evaluated for canonical memory markers at day 30 after 3° short-term and long-term boosting. Memory precursor effector cells (MPECs), effector CD8 T cells which give rise to memory T cells, are defined by expression of the IL-7 receptor α chain, CD127, and lack of killer cell lectin-like receptor subfamily G member 1 (KLRG1) expression (34, 35). At day 30 after 3°, approximately half of the short-boosted K^b-

SIINFEKL-specific CD8 T cells are positive for CD127, but not KLRG1, thus displaying a classic MPEC phenotype (Figures 5A-B). This is a significantly higher percentage of MPECs than in long-boosted T cells, as the majority of long-term boosted K^b-SIINFEKL-specific CD8 T cells (~70%) are positive for both CD127 and KLRG1 (Figures 5A,C). Per cell expression of CD127, as measured by geometric mean fluorescence intensity (GMFI), indicated similar levels of CD127 on short- and long-boosted Ag-specific CD8 T cells (Figure 5D).

Other canonical memory markers such as the IL-15 receptor β chain, CD122, the IL-2 receptor α chain, CD25, and a member of the tumor necrosis factor receptor superfamily, CD27, were all similarly expressed between short-boosted and long-boosted K^b-SIINFEKL-specific CD8 T cells. The expression of the transcription factor T-bet was also similar on short- and long-boosted T cells. While Eomes protein appears decreased on short-boosted Ag-specific T cells in comparison to long-term boosted cells, this is not statistically significant when comparing GMFI (data not shown). Bcl-2, an anti-apoptotic marker, is comparable in short- and long-term boosted K^b-SIINFEKL-specific CD8 T cells. Despite shortening the time between immunizations to 2 week intervals, short-boosted K^b-SIINFEKL-specific CD8 T cells were not PD-1 high, indicating that short HPBB does not drive a phenotype associated with T cell exhaustion (Figure 5D). These data demonstrate that shortening the gap between immunizations did not alter the acquisition of canonical memory markers by Ag-specific CD8 T cells.

Short-boosted Ag-specific CD8 T cells display altered metabolic properties compared to long-term boosted T cells

The metabolic activity of memory CD8 T cells has been linked to their function and survival (32, 36–40). Oxidative phosphorylation has been shown to be a dominant metabolic pathway for memory CD8 T cells (41, 42). Compared to naïve and effector T cells, memory T cells maintain a significantly higher spare respiratory capacity (SRC), which is important to their establishment and rapid recall response to reinfection (38, 40). SRC is the reserve capacity of cells to make energy in response to increased stress or work (43). Since both short-boosted and long-boosted T cells displayed phenotypic markers associated with long-term memory, we investigated whether short- and long-boosted CD8 T cells exhibited similar metabolic signatures. To evaluate this, the oxygen consumption rate (OCR), an indicator of oxidative phosphorylation, of Ag-specific CD8 T cells under different cell stressors was measured in purified K^b-SIINFEKL-specific CD8 T cells at days 30, 51 and 69 following the 3° boost using the Seahorse platform (Figure 6). This assay uses compounds that specifically target electron transport chain components to disrupt cellular respiration (32, 38). OCR was measured at basal conditions and after the addition of each of the indicated metabolic inhibitors to assess metabolic function. Oligomycin and rotenone addition measure ATP-linked respiration and non-mitochondrial respiration, respectively. The addition of FCCP, which uncouples the electron transport chain, allows for measuring maximum OCR (Figure 6A). From this, SRC can be calculated, which is the corrected basal OCR subtracted from corrected maximum OCR (32). Our analysis revealed reduction in maximal OCR in short-boosted K^b-SIINFEKL-specific CD8 T cells compared to long-boosted T cells at day 30 (Figure 6). By day 51 after 3°, short-boosted Ag-specific cells still

exhibited lower maximal OCR compared to long-boosted K^b-SIINFEKL-specific CD8 T cells, but this difference was not statistically significant (Figures 6B-C). At day 69 after 3° boosting, there was no metabolic differences observed between short- and long-boosted Ag-specific CD8 T cells (Figures 6B-C). At all time points, basal OCR and SCR was not statistically different between short- and long-boosted K^b-SIINFEKL-specific CD8 T cells although SCR was decreased in comparison to long-boosted T cells at day 30 and 51 (Figures 6A,C and data not shown). In summary, short-boost-derived memory CD8 T cells exhibited metabolic differences as compared to long-boosted cells, but only at earlier memory timepoints.

Ag-specific CD8 T cells generated through short-boosting contract without stabilization, despite displaying a memory phenotype

Metabolic differences between short-boosted and long-boosted K^b-SIINFEKL-specific CD8 T cells at early memory timepoints indicated potential disparities in the ability of short-boosted T cells to establish stable memory. To evaluate whether short-boosting and long-boosting vaccine regimens result in the formation of memory CD8 T cells of similar quantity and longevity, K^b-SIINFEKL-specific CD8 T cell responses were evaluated in the spleen over 134 days following 3° vaccination (Figure 7). At an effector timepoint after 3° boost (days 5-14), numbers of Ag-specific CD8 T cells generated by short- or long-boosting intervals were not statistically different with ~8×10^6 and 1×10^7 cells, respectively (Figure 7B). Long-term boosted K^b-SIINFEKL-specific CD8 T cells were stably maintained after 3°, at least for 117 days, which was the last timepoint. In contrast, K^b-SIINFEKL-specific CD8 T cells generated with short-boosting intervals contracted significantly by day 30 after 3° vaccination and this population continued to decline over 134 days. The number of Ag-specific CD8 T cells enumerated at 134 days after short-boosting was nearly 12-fold lower than cells at an effector time point, whereas long-boosted K^b-SIINFEKL-specific CD8 T cells showed little contraction (Figure 7B). Thus, short-boosted CD8 T cells are not stably maintained in the absence of Ag compared to cells generated by longer intervals between immunizations.

Discussion

CD8 T cells contribute to protection against many infections and efficacious CD8 T cell memory may be particularly important to eliminate certain pathogens. Vaccine strategies should generate high quality memory CD8 T cells that can rapidly purge the offending organism from the host and ideally, vaccination would afford almost immediate protection. Heterologous prime-boost-boost (HPBB) is a multi-step immunization scheme, which has the remarkable feature of forming high quantities of stable memory CD8 T cells (12, 13). However, boosting intervals are long, meaning that vaccination is not complete for several months (14, 15). Thus, in this study we investigated how the quality, quantity and location of Ag-specific CD8 T cells is affected by decreasing the time between boosting events. It has been previously demonstrated that expression of CCL21, the ligand for CCR7, is downregulated during different microbial infections, including lymphocytic choriomeningitis virus (LCMV), LM and VV. This leads to altered migration and priming of T cells. Chemokine downregulation is transient and, by day 14 after infection, CCL21 levels

are back to pre-infection concentrations (44). Therefore, we chose 14 days as the resting period between boosting events to allow animals to regain some immune homeostasis. We show that condensing the intervals between boosting results in functional and protective Ag-specific CD8 T cells in 4 weeks.

We discovered that Ag-specific CD8 T cell numbers early after each vaccination step increase within peripheral blood lymphocytes (PBL), spleen and small intestinal intraepithelial lymphocytes (IEL) (Figure 1). Indeed up to 62% of CD8 T cells were K^b-SIINFEKL-specific in PBL by day 14 after the final boost. Short HPBB also led to memory T cell populations in the lungs, liver, female reproductive tract (FRT) and salivary gland (SG) that comprise up to 40% of CD8 T cells. Thus, short HPBB can generate large populations of Ag-specific CD8 T cells through out the host.

A concern was that this curtailed immunization schedule may have induced a state of exhaustion or non-responsiveness in K^b-SIINFEKL-specific CD8 T cells. However, the 3° recall was robust and short-boosted T cells were able to protect against infection as efficiently as long-boosted T cells (Figures 1,3,4). All K^b-SIINFEKL-specific CD8 T cells at day 14 post 3° produced cytokines and were not PD-1 high (Figures 4B, 5D), other indicators that these T cells were not exhausted. Furthermore, Ag-specific CD8 T cells generated through short-boosting have similar proliferative capabilities compared to long-term boosted T cells (Figure 4C-E). Therefore, the 14-day intervals between immunizations did not induce functional defects associated with overexposure to an inflammatory microbial environment. This may be expected, as there appears to be a window of opportunity for the induction of exhaustion, which necessitates prolonged exposure to this environment. When CD8 T cells specific for chronic LCMV clone-13 are transferred at day 8 after infection to a naïve, uninfected new host, certain hallmarks of T cell exhaustion are prevented (45).

Many infections begin at mucosal surfaces. CD8 T cell mediated killing requires direct contact with target cells and vaccines must position CD8 T cells at the site of infection. The recently described CD8 T cell memory subset, tissue resident memory T cells (T_{RM}), are uniquely positioned to act as immediate sentinels of re-infection, setting up an anti-microbial state (10, 11). As precise localization of T cells within tissue compartments can be complicated by vascularization, we used an intravascular staining technique to discriminate cell localization between the tissue parenchyma or tissue vasculature (28). We found that short-term HPBB drives T cell migration to the parenchyma in multiple non-lymphoid tissues (NLT), which are populated for at least 95 days after the last immunization (Figures 2C-D). The CD62L low phenotype of these cells indicates that the majority of cells in the tissue generated from short-boosting are likely T_{EM} cells, which is in line with what has been shown for HPBB with long-boosting intervals in secondary lymphoid organs (46). However, a significant fraction of cells in the IEL and SG are CD69 positive and CD103 positive suggesting that they are T_{RM} (Supplementary Figure 1) (29, 47, 48). Generating CD8 T cells with a T_{RM} phenotype may be particularly important for vaccination, as this cell type has been shown to be critical in providing protection during re-infection (10, 11, 49). It was recently shown that CD8 T cell quantity has been underappreciated, particularly in NLT, due to sub-optimal tissue disruption and lymphocyte isolation techniques and that

CD103/CD69 phenotyping may not label all T_{RM} (29). Thus, it is likely that the numbers of K^b-SIINFEKL-specific CD8 T_{RM} cells are higher than what we have observed herein.

Formation of a stable population of memory CD8 T cells is important for a vaccine to achieve long-term protection. CD127 expression on Ag-specific CD8 T cells has been shown to predict memory precursor effector cells (MPECs), which go on to become memory T cells (34). MPECs have also been shown to lack expression of KLRG1 (35). Given the brevity of rest periods between immunizations, short-boosted CD8 T cells would have been predicted to be terminally differentiated, but based on phenotype, these appear to be optimal memory CD8 T cells. In fact, a greater percent of short-boosted tetramer+ CD8 T cells were positive for CD127 and negative for KLRG1, as compared to long-boosted T cells (Figures 5A-C). Therefore, it was surprising to discover that the short-boosted K^b-SIINFEKL-specific CD8 T cells continuously eroded over a 134-day timespan (Figure 7). It might have been expected that short-boosted T cells would display a short-lived effector cell phenotype of KLRG1 positive, CD127 negative, but this was not the case. Interestingly, exhausted CD8 T cells, which have a loss of memory potential, lack expression of KLRG1 during chronic LCMV clone 13, indicating that absence of KLRG1 expression is not always associated with T cell longevity (45).

T-bet and Eomes have been shown to impact CD127 and KLRG1 expression in effector CD8 T cells, where high Eomes and low T-bet expression induces a KLRG1 low, CD127 high population of CD8 T cells that is maintained into memory (35, 50–52). However, in our study, expression of T-bet and Eomes was similar between short- and long-boosted populations despite their disparate longevity. Short-boosted Ag-specific CD8 T cells also express similar levels of CD27, CD122, CD25 and Bcl-2 as compared to long-boosted T cells, indicating that they are capable of receiving survival signals via these molecules, but they fail to be maintained equally (Figure 5D). This incongruity suggests that there are other factors, contributing to the decay of short-boosted CD8 T cells that can overcome a signature indicative of long-lived memory T cells.

The metabolism of CD8 T cells is important in memory cell function and survival (32, 36–40). Oxidative phosphorylation supports the metabolic needs of memory CD8 T cells, while glycolysis supports effector T cells (41, 42). To this end, the spare respiratory capacity (SRC) of memory CD8 T cells has been shown to be greater than that of naive and effector CD8 T cells and is thought to regulate memory CD8 T cell formation and functionality (38). Therefore, it was surprising, given the continuous contraction of short-boosted CD8 T cells, that SRC was not statistically different between short- and long-boosted T cells (Figure 6C). However, short-boosted Ag-specific CD8 T cells have a significantly lower maximal oxygen consumption rate (OCR) compared to long-boosted T cells at day 30 (Figure 6). This might have deleterious effects on longevity, even though recall responses were not affected (Figure 4). Perhaps shortening boost intervals does not give ample time for cells to become bioenergetically stable between immunizations. This is supported by the recent finding that the mitochondrial function of CD8 T cells increases with time after infection (53). One interpretation is that short HPBB generates a mixed population of cells differing in their mitochondrial capacity. Less metabolically fit Ag-specific CD8 T cells may dominate the response early after 3° immunization and rely more heavily on glycolysis during steady state

conditions. As the inflammatory environment subsides and growth factors are reduced, these cells may preferentially die over time leaving a more stable memory cell population to survive long-term. This could explain the reduced, but not significant, SRC of short-boosted K^b-SIINFEKL-specific CD8 T cells at day 30 and 51 after 3°, whereby some T cells are able to function at higher SRC than others. Indeed, the contraction of short-boosted Ag-specific CD8 T cells slows substantially around day 60 after 3° (Figure 7B). This slowed contraction may be explained by the identical metabolic activity of short- and long-boosted K^b-SIINFEKL-specific CD8 T cells observed at day 69 after 3° (Figures 6B-C).

Interestingly, studies show that T cells that take up high amounts of glucose exhibit the molecular profile of short-lived effector cells (37). We show here a different phenomenon: metabolic alterations of T cells that display a memory phenotype, but do not form stable numbers of memory T cells (Figures 5 and 7). Further investigation of the metabolic pathway and energy consumption by CD8 T cells generated through short-boosting would be needed to reveal if metabolism is directly contributing to memory T cell contraction. Regardless of metabolic activity and continued contraction, short-boosted T cells are able to respond to infection at any time point measured after 3° comparably to long-boosted mice (Figure 4). This further supports our conclusions that functionality is not compromised following short-boosting, even at late memory timepoints (Figure 4D).

Our study shows that shortening the boosting intervals during HPBB will generate Ag-specific CD8 T cells that are functional and protective. While these CD8 T cells gradually decay in number, they are still able to proliferate and respond to infection comparably to long-boosted T cells. Despite protracted contraction, the population of short-boosted CD8 T cells remaining after 3° is still greater than the population remaining after 1° and 2° boosts, indicating that short HPBB is still advantageous over single boosts. Overall, shortening boosting intervals preserves the function of Ag-specific CD8 T cells, despite ongoing contraction, and could be useful in situations where protection needs to be achieved rapidly.

Supplementary Material

Refer to Web version on PubMed Central for supplementary material.

Acknowledgements

We thank Dr. David Masopust for discussion and critical reading of the manuscript and Dr. Kathryn Fraser and Eric Hanse for discussion of metabolic assays.

This work was supported by the National Institutes of Health grant DP2OD006472 (to V.V.) and the National Institutes of Health Immunology grant T32AI007313 (to E.A.T. and C.E.N.)

Glossary

FRT	female reproductive tract
HPBB	heterologous prime-boost-boost
IEL	intraepithelial lymphocytes

IgLN	inguinal lymph node
KLRG1	killer cell lectin-like receptor subfamily F
LM	*Listeria monocytogenes*
LN	lymph node
NLT	non-lymphoid tissue
OCR	oxygen consumption rate
SG	salivary gland
SRC	spare respiratory capacity
VSV	vesicular stomatitis virus
VV	vaccinia virus

References

1. Seder RA, Chang L-J, Enama ME, Zephir KL, Sarwar UN, Gordon IJ, Holman LA, James ER, Billingsley PF, Gunasekera A, Richman A, Chakravarty S, Manoj A, Velmurugan S, Li M, Ruben AJ, Li T, Eappen AG, Stafford RE, Plummer SH, Hendel CS, Novik L, Costner PJM, Mendoza FH, Saunders JG, Nason MC, Richardson JH, Murphy J, Davidson SA, Richie TL, Sedegah M, Sutamihardja A, Fahle GA, Lyke KE, Laurens MB, Roederer M, Tewari K, Epstein JE, Sim BKL, Ledgerwood JE, Graham BS, Hoffman SL, the V. 312 S. Team. DiGiovanni C, Williams P, Luongo N, Mitchell J, Florez MB, Larkin B, Berkowitz N, Wilson B, Clarke T, Vasilenko O, Yamshchikov G, Sitar S, Stanford L, Pittman I, Bailer RT, Casazza J, Decederfelt H, Starling J, Williams EC, Lau A, Antonara S, Brocious J, Kemp M, Inglese J, Dranchak P, Abot EN, Reyes S, Ganeshan H, Belmonte M, Huang J, Belmonte A, Komisar J, Abebe Y, Getachew Y, Patil A, Matheny S, Nelson K, Overby J, Pich V, Wen Y, Fan R, Fomumbod E, Awe A, Chakiath C, King M, Orozco MS, Murshedkar T, Padilla D, Jiang B, Gao L, Kc N, Xu R, Adams M, Plowe C, Loblein H, Renehan PZ, Kunchai M, Diep L. Protection Against Malaria by Intravenous Immunization with a Nonreplicating Sporozoite Vaccine. Science. 2013; 341:1359–1365. [PubMed: 23929949]
2. Koup RA, Douek DC. Vaccine Design for CD8 T Lymphocyte Responses. Cold Spring Harb. Perspect. Med. 2011:1.
3. Shoukry NH, Grakoui A, Houghton M, Chien DY, Ghrayeb J, Reimann KA, Walker CM. Memory CD8+ T cells are required for protection from persistent hepatitis C virus infection. J. Exp. Med. 2003; 197:1645–1655. [PubMed: 12810686]
4. Brown LE, Kelso A. Prospects for an influenza vaccine that induces cross-protective cytotoxic T lymphocytes. Immunol. Cell Biol. 2009; 87:300–308. [PubMed: 19308073]
5. Woodworth JSM, Behar SM. Mycobacterium tuberculosis specific CD8+ T cells and their role in immunity. Crit. Rev. Immunol. 2006; 26:317–352. [PubMed: 17073557]
6. Reyes-Sandoval A, Berthoud T, Alder N, Siani L, Gilbert SC, Nicosia A, Colloca S, Cortese R, Hill AVS. Prime-Boost Immunization with Adenoviral and Modified Vaccinia Virus Ankara Vectors Enhances the Durability and Polyfunctionality of Protective Malaria CD8+ T-Cell Responses. Infect. Immun. 2010; 78:145–153. [PubMed: 19858306]
7. Obar JJ, Lefrançois L. Memory CD8+ T cell differentiation. Ann. N. Y. Acad. Sci. 2010; 1183:251–266. [PubMed: 20146720]
8. Wherry EJ, Teichgräber V, Becker TC, Masopust D, Kaech SM, Antia R, von Andrian UH, Ahmed R. Lineage relationship and protective immunity of memory CD8 T cell subsets. Nat. Immunol. 2003; 4:225–234. [PubMed: 12563257]

9. Sallusto F, Geginat J, Lanzavecchia A. Central memory and effector memory T cell subsets: function, generation, and maintenance. Annu. Rev. Immunol. 2004; 22:745–763. [PubMed: 15032595]
10. Schenkel JM, Fraser KA, Beura LK, Pauken KE, Vezys V, Masopust D. Resident memory CD8 T cells trigger protective innate and adaptive immune responses. Science. 2014; 346:98–101. [PubMed: 25170049]
11. Ariotti S, Hogenbirk MA, Dijkgraaf FE, Visser LL, Hoekstra ME, Song J-Y, Jacobs H, Haanen JB, Schumacher TN. Skin-resident memory CD8+ T cells trigger a state of tissue-wide pathogen alert. Science. 2014; 346:101–105. [PubMed: 25278612]
12. Fraser KA, Schenkel JM, Jameson SC, Vezys V, Masopust D. Preexisting High Frequencies of Memory CD8+ T Cells Favor Rapid Memory Differentiation and Preservation of Proliferative Potential upon Boosting. Immunity. 2013; 39:171–183. [PubMed: 23890070]
13. Masopust D, Ha S-J, Vezys V, Ahmed R. Stimulation history dictates memory CD8 T cell phenotype: implications for prime-boost vaccination. J. Immunol. Baltim. Md 1950. 2006; 177:831–839.
14. Woodland DL. Jump-starting the immune system: prime–boosting comes of age. Trends Immunol. 2004; 25:98–104. [PubMed: 15102369]
15. Lu S. Heterologous prime-boost vaccination. Curr. Opin. Immunol. 2009; 21:346–351. [PubMed: 19500964]
16. Akande TM, A SA. A Study of Compliance to Hepatitis B Vaccination Among Health Workers in a Tertiary Health Institution. Hosp. Pract. 2010; 5:13–16.
17. Van Herck K, Leuridan E, Van Damme P. Schedules for hepatitis B vaccination of risk groups: balancing immunogenicity and compliance. Sex. Transm. Infect. 2007; 83:426–432. [PubMed: 17911142]
18. Luman ET, Shaw KM, Stokley SK. Compliance with vaccination recommendations for U.S. children. Am. J. Prev. Med. 2008; 34:463–470. [PubMed: 18471581]
19. Nelson JC, Bittner RCL, Bounds L, Zhao S, Baggs J, Donahue JG, Hambidge SJ, Jacobsen SJ, Klein NP, Naleway AL, Zangwill KM, Jackson LA. Compliance with multiple-dose vaccine schedules among older children, adolescents, and adults: results from a vaccine safety datalink study. Am. J. Public Health. 2009; 99(Suppl 2):S389–397. [PubMed: 19797753]
20. Slütter B, Pewe LL, Lauer P, Harty JT. Cutting Edge: Rapid Boosting of Cross-Reactive Memory CD8 T Cells Broadens the Protective Capacity of the Flumist Vaccine. J. Immunol. 2013; 190:3854–3858. [PubMed: 23467935]
21. Wong P, Lara-Tejero M, Ploss A, Leiner I, Pamer EG. Rapid Development of T Cell Memory. J. Immunol. 2004; 172:7239–7245. [PubMed: 15187098]
22. Bridle BW, Boudreau JE, Lichty BD, Brunellière J, Stephenson K, Koshy S, Bramson JL, Wan Y. Vesicular Stomatitis Virus as a Novel Cancer Vaccine Vector to Prime Antitumor Immunity Amenable to Rapid Boosting With Adenovirus. Mol. Ther. 2009; 17:1814–1821. [PubMed: 19603003]
23. Pham N-LL, Pewe LL, Fleenor CJ, Langlois RA, Legge KL, Badovinac VP, Harty JT. Exploiting cross-priming to generate protective CD8 T-cell immunity rapidly. Proc. Natl. Acad. Sci. U. S. A. 2010; 107:12198–12203. [PubMed: 20616089]
24. Badovinac VP, Harty JT. Manipulating the Rate of Memory CD8+ T Cell Generation after Acute Infection. J. Immunol. 2007; 179:53–63. [PubMed: 17579021]
25. Shen H, Slifka MK, Matloubian M, Jensen ER, Ahmed R, Miller JF. Recombinant Listeria monocytogenes as a live vaccine vehicle for the induction of protective anti-viral cell-mediated immunity. Proc. Natl. Acad. Sci. U. S. A. 1995; 92:3987–3991. [PubMed: 7732018]
26. Restifo NP, Bačík I, Irvine KR, Yewdell JW, McCabe BJ, Anderson RW, Eisenlohr LC, Rosenberg SA, Bennink JR. Antigen Processing In Vivo and the Elicitation of Primary CTL Responses. J. Immunol. Baltim. Md 1950. 1995; 154:4414–4422.
27. Kim S-K, Reed DS, Olson S, Schnell MJ, Rose JK, Morton PA, Lefrançois L. Generation of mucosal cytotoxic T cells against soluble protein by tissue-specific environmental and costimulatory signals. Proc. Natl. Acad. Sci. U. S. A. 1998; 95:10814–10819. [PubMed: 9724787]

28. Anderson KG, Mayer-Barber K, Sung H, Beura L, James BR, Taylor JJ, Qunaj L, Griffith TS, Vezys V, Barber DL, Masopust D. Intravascular staining for discrimination of vascular and tissue leukocytes. Nat. Protoc. 2014; 9:209–222. [PubMed: 24385150]
29. Steinert EM, Schenkel JM, Fraser KA, Beura LK, Manlove LS, Igyártó BZ, Southern PJ, Masopust D. Quantifying Memory CD8 T Cells Reveals Regionalization of Immunosurveillance. Cell. 2015; 161:737–749. [PubMed: 25957682]
30. Beura LK, Anderson KG, Schenkel JM, Locquiao JJ, Fraser KA, Vezys V, Pepper M, Masopust D. Lymphocytic choriomeningitis virus persistence promotes effector-like memory differentiation and enhances mucosal T cell distribution. J. Leukoc. Biol. 2015; 97:217–225. [PubMed: 25395301]
31. Earl PL, Cooper N, Wyatt LS, Moss B, Carroll MW. Preparation of cell cultures and vaccinia virus stocks. Curr. Protoc. Mol. Biol. Ed. Frederick M Ausubel Al. 2001 Chapter 16: Unit16.16.
32. Gubser PM, Bantug GR, Razik L, Fischer M, Dimeloe S, Hoenger G, Durovic B, Jauch A, Hess C. Rapid effector function of memory CD8+ T cells requires an immediate-early glycolytic switch. Nat. Immunol. 2013; 14:1064–1072. [PubMed: 23955661]
33. Masopust D, Vezys V, Marzo AL, Lefrançois L. Preferential Localization of Effector Memory Cells in Nonlymphoid Tissue. Science. 2001; 291:2413–2417. [PubMed: 11264538]
34. Kaech SM, Tan JT, Wherry EJ, Konieczny BT, Surh CD, Ahmed R. Selective expression of the interleukin 7 receptor identifies effector CD8 T cells that give rise to long-lived memory cells. Nat. Immunol. 2003; 4:1191–1198. [PubMed: 14625547]
35. Joshi NS, Cui W, Chandele A, Lee HK, Urso DR, Hagman J, Gapin L, Kaech SM. Inflammation directs memory precursor and short-lived effector CD8(+) T cell fates via the graded expression of T-bet transcription factor. Immunity. 2007; 27:281–295. [PubMed: 17723218]
36. Rao RR, Li Q, Odunsi K, Shrikant PA. The mTOR kinase determines effector versus memory CD8+ T cell fate by regulating the expression of transcription factors T-bet and Eomesodermin. Immunity. 2010; 32:67–78. [PubMed: 20060330]
37. Sukumar M, Liu J, Ji Y, Subramanian M, Crompton JG, Yu Z, Roychoudhuri R, Palmer DC, Muranski P, Karoly ED, Mohney RP, Klebanoff CA, Lal A, Finkel T, Restifo NP, Gattinoni L. Inhibiting glycolytic metabolism enhances CD8+ T cell memory and antitumor function. J. Clin. Invest. 2013; 123:4479–4488. [PubMed: 24091329]
38. van der Windt GJW, Everts B, Chang C-H, Curtis JD, Freitas TC, Amiel E, Pearce EJ, Pearce EL. Mitochondrial Respiratory Capacity Is a Critical Regulator of CD8+ T Cell Memory Development. Immunity. 2012; 36:68–78. [PubMed: 22206904]
39. Pearce EL, Walsh MC, Cejas PJ, Harms GM, Shen H, Wang L-S, Jones RG, Choi Y. Enhancing CD8 T Cell Memory by Modulating Fatty Acid Metabolism. Nature. 2009; 460:103–107. [PubMed: 19494812]
40. van der Windt GJW, O'Sullivan D, Everts B, Huang SC-C, Buck MD, Curtis JD, Chang C-H, Smith AM, Ai T, Faubert B, Jones RG, Pearce EJ, Pearce EL. CD8 memory T cells have a bioenergetic advantage that underlies their rapid recall ability. Proc. Natl. Acad. Sci. U. S. A. 2013; 110:14336–14341. [PubMed: 23940348]
41. van der Windt GJW, Pearce EL. Metabolic switching and fuel choice during T-cell differentiation and memory development. Immunol. Rev. 2012; 249:27–42. [PubMed: 22889213]
42. Fox CJ, Hammerman PS, Thompson CB. Fuel feeds function: energy metabolism and the T-cell response. Nat. Rev. Immunol. 2005; 5:844–852. [PubMed: 16239903]
43. Nicholls DG. Spare respiratory capacity, oxidative stress and excitotoxicity. Biochem. Soc. Trans. 2009; 37:1385–1388. [PubMed: 19909281]
44. Mueller SN, Hosiawa-Meagher KA, Konieczny BT, Sullivan BM, Bachmann MF, Locksley RM, Ahmed R, Matloubian M. Regulation of Homeostatic Chemokine Expression and Cell Trafficking During Immune Responses. Science. 2007; 317:670–674. [PubMed: 17673664]
45. Angelosanto JM, Blackburn SD, Crawford A, Wherry EJ. Progressive Loss of Memory T Cell Potential and Commitment to Exhaustion during Chronic Viral Infection. J. Virol. 2012; 86:8161–8170. [PubMed: 22623779]

46. Vezys V, Yates A, Casey KA, Lanier G, Ahmed R, Antia R, Masopust D. Memory CD8 T-cell compartment grows in size with immunological experience. Nature. 2009; 457:196–199. [PubMed: 19005468]

47. Casey KA, Fraser KA, Schenkel JM, Moran A, Abt MC, Beura LK, Lucas PJ, Artis D, Wherry EJ, Hogquist K, Vezys V, Masopust D. Antigen-independent differentiation and maintenance of effector-like resident memory T cells in tissues. J. Immunol. Baltim. Md 1950. 2012; 188:4866–4875.

48. Masopust D, Choo D, Vezys V, Wherry EJ, Duraiswamy J, Akondy R, Wang J, Casey KA, Barber DL, Kawamura KS, Fraser KA, Webby RJ, Brinkmann V, Butcher EC, Newell KA, Ahmed R. Dynamic T cell migration program provides resident memory within intestinal epithelium. J. Exp. Med. 2010; 207:553–564. [PubMed: 20156972]

49. Jiang X, Clark RA, Liu L, Wagers AJ, Fuhlbrigge RC, Kupper TS. Skin infection generates non-migratory memory CD8+ T(RM) cells providing global skin immunity. Nature. 2012; 483:227–231. [PubMed: 22388819]

50. Kaech SM, Cui W. Transcriptional control of effector and memory CD8+ T cell differentiation. Nat. Rev. Immunol. 2012; 12:749–761. [PubMed: 23080391]

51. Intlekofer AM, Takemoto N, Kao C, Banerjee A, Schambach F, Northrop JK, Shen H, Wherry EJ, Reiner SL. Requirement for T-bet in the aberrant differentiation of unhelped memory CD8+ T cells. J. Exp. Med. 2007; 204:2015–2021. [PubMed: 17698591]

52. Intlekofer AM, Takemoto N, Wherry EJ, Longworth SA, Northrup JT, Palanivel VR, Mullen AC, Gasink CR, Kaech SM, Miller JD, Gapin L, Ryan K, Russ AP, Lindsten T, Orange JS, Goldrath AW, Ahmed R, Reiner SL. Effector and memory CD8+ T cell fate coupled by T-bet and eomesodermin. Nat. Immunol. 2005; 6:1236–1244. [PubMed: 16273099]

53. Martin MD, Kim MT, Shan Q, Sompallae R, Xue H-H, Harty JT, Badovinac VP. Phenotypic and Functional Alterations in Circulating Memory CD8 T Cells with Time after Primary Infection. PLoS Pathog. 2015; 11:e1005219. [PubMed: 26485703]

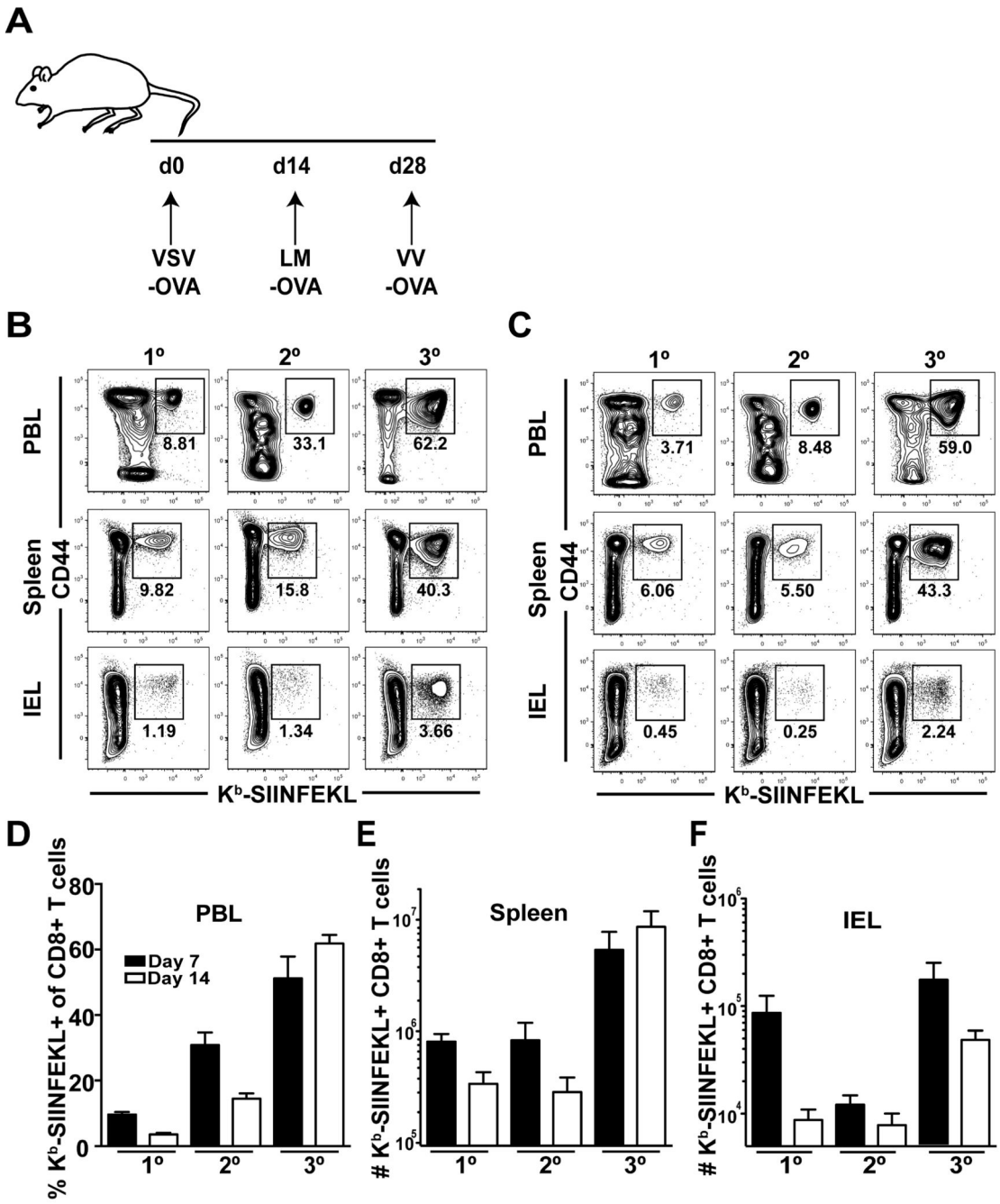

FIGURE 1. Short-boosting intervals generate large numbers of Ag-specific CD8 T cells

(A) Short-boosting immunization regimen. Boosts occurred 14 days apart. (B, C) Peripheral blood lymphocytes (PBL), spleen, and small intestinal intraepithelial lymphocytes (IEL) were analyzed (B) 7 days or (C) 14 days after 1°, 2° or 3° boosting. Plots are gated on CD8 T cells. (D) Percent of CD44+ K^b-SIINFEKL+ CD8 T cells in PBL at day 7 (black) and 14 (white) after 1°, 2° or 3° boosting. (E-F) Number of CD44+ K^b-SIINFEKL+ CD8 T cells in spleen (E) and IEL (F) at day 7 (black) or day 14 (white) following 1°, 2° or 3° boosting. Data are representative of 2 experiments, N=3 mice per experiment.

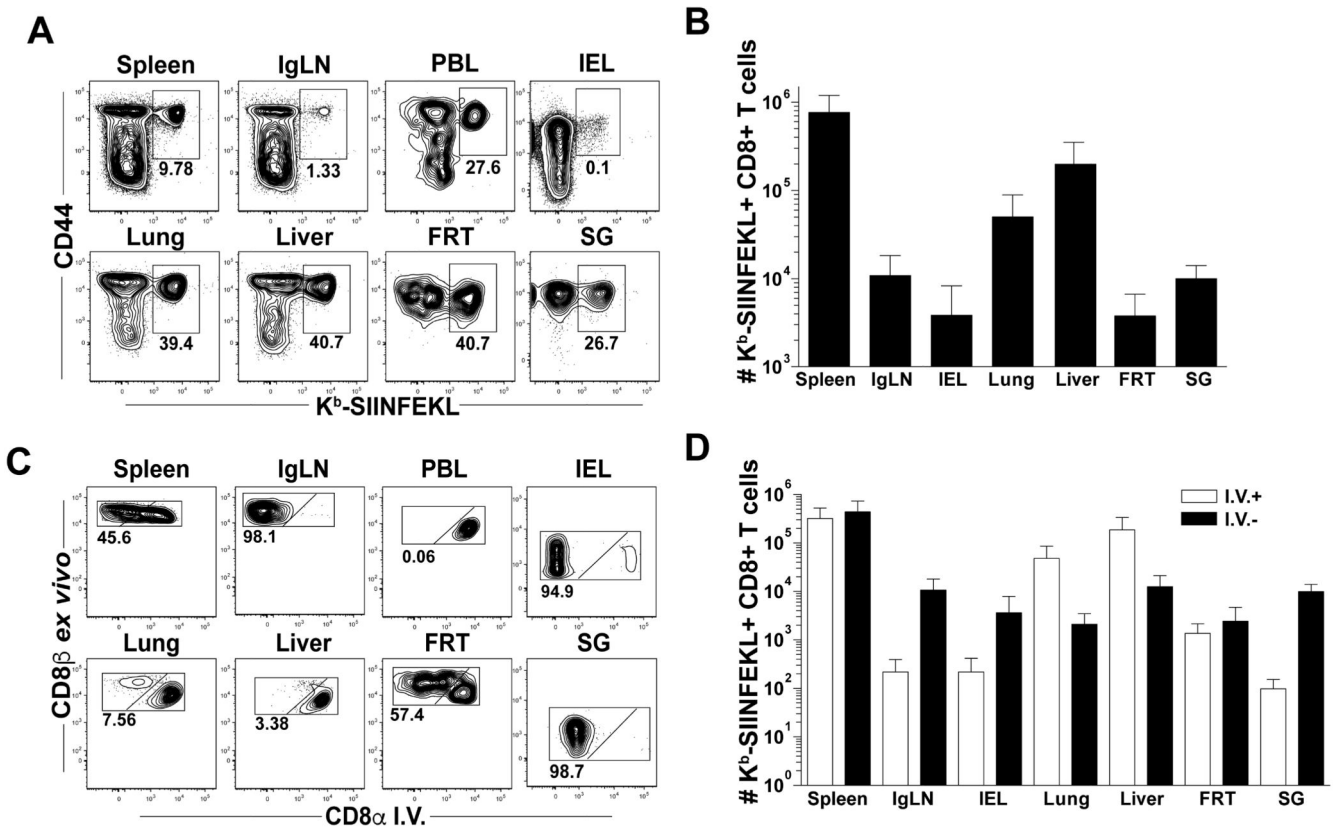

FIGURE 2. Short-boosted Ag-specific CD8 T cells migrate to and populate multiple non-lymphoid tissues

Splenocytes, inguinal lymph nodes (IgLN), peripheral blood lymphocytes (PBL), small intestinal intraepithelial lymphocytes (IEL), lung, liver, female reproductive tract (FRT) and salivary gland (SG) lymphocytes were isolated at least 95 days after 3° infection. (A) Plots are gated on CD8+ T cells. (B) Quantification of K^b-SIINFEKL+ CD8 T cells as in (A). (C-D) Mice were injected with anti-CD8α Ab i.v. to identify the precise localization of T cells within the tissue parenchyma (I.V.-) or within the tissue vasculature (I.V.+). (C) Representative flow plots gated on CD44+ K^b-SIINFEKL+ CD8 T cells. (D) Quantification of K^b-SIINFEKL+ CD8 T cells as in (C). Data are representative of 2 experiments, at least N=3 mice per experiment except IEL and SG where is N=3 total.

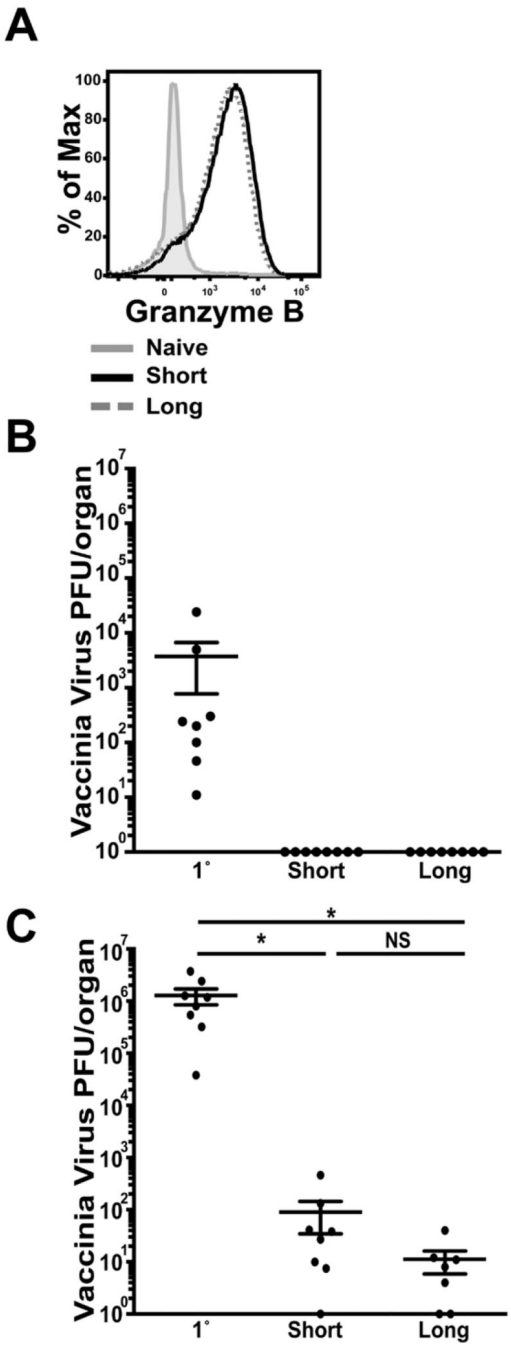

FIGURE 3. Short-boosted Ag-specific CD8 T cells express granzyme B and protect against viral infection

(A) Splenocytes were isolated at day 5 post 3°. Granzyme B expression is shown on CD44+ K^b-SIINFEKL-specific CD8 T cells from short-boosted mice (black, solid line) and long-boosted mice (grey, dashed line); grey filled histogram indicates gating on CD44 low CD8+ T cells. (B) Spleen and (C) ovaries from 3° short-boosted, 3° long-boosted or 1° VV-OVA challenged mice were isolated at day 5 after VV-OVA to determine vaccinia virus titers. Data are representative of 2 experiments, N=3-4 mice per experiment. Graphs show mean +/− SEM. * = $p<0.05$.

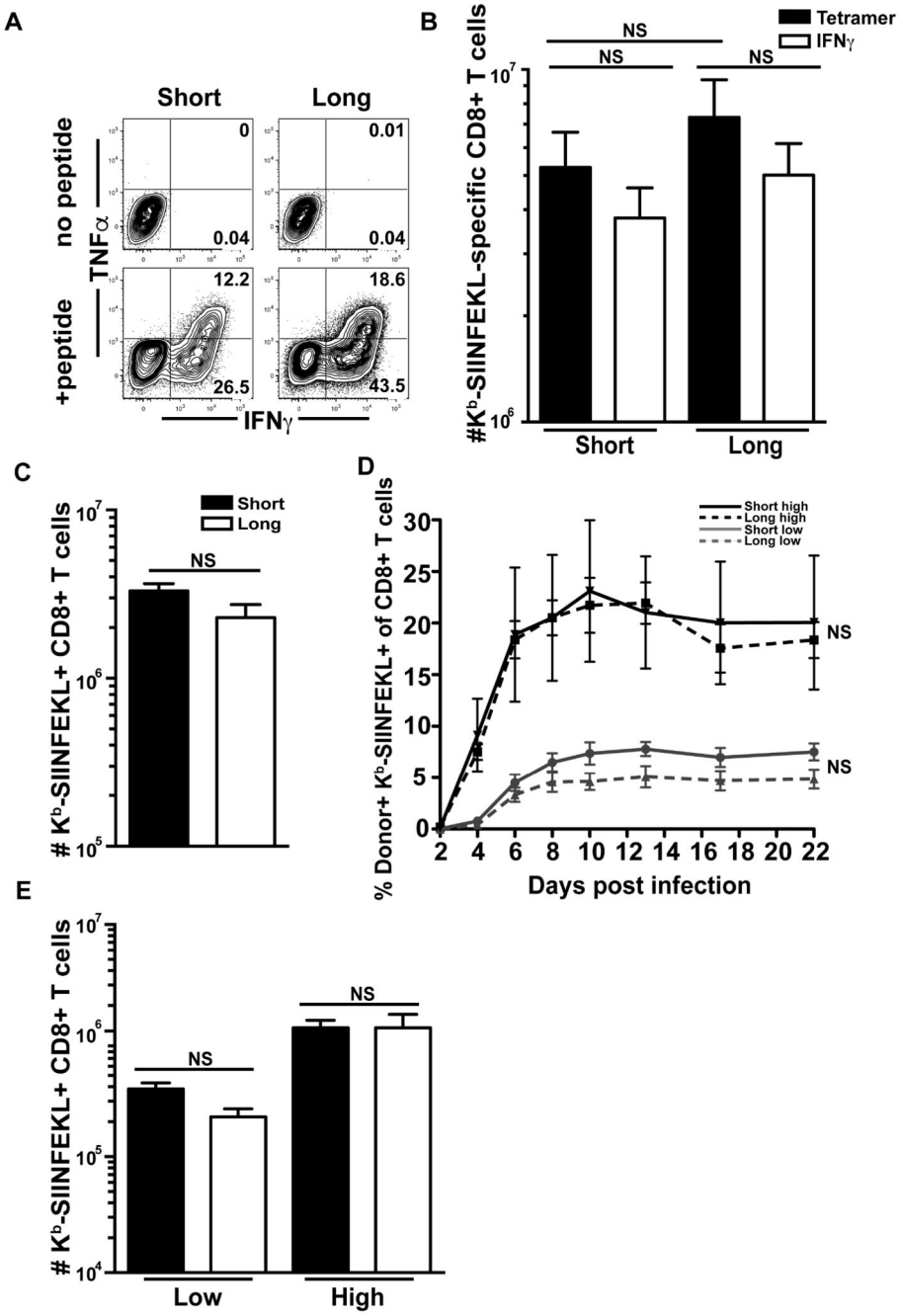

FIGURE 4. Short-boosted Ag-specific CD8 T cells are functional

(A) Splenocytes from short-boosted or long-boosted mice were stimulated at day 14 after 3° HPBB with or without SIINFEKL peptide and examined for TNFα and IFNγ production. Plots are gated on CD8+ T cells. (B) K^b-SIINFEKL tetramer+ CD8 T cells (black) and IFNγ -producing CD8 T cells (white) were enumerated in spleen at day 14 post 3°. Data are representative of 2 experiments N=1-5 mice per experiment. (C) Splenocytes were isolated 32 days post 3° from short- and long-boosted mice, enriched for CD8 T cells and equal numbers of K^b-SIINFEKL-specific CD8 T cells were transferred to naïve CD45.1 mice.

New hosts were infected with VSV-OVA 1 day after transfer. 6 days after infection, the number of donor+, K^b-SIINFEKL+ CD8 T cells was enumerated in spleen. Data are representative of 1 experiment, N= 6-7. (D) Splenocytes were isolated at day 95 post 3° from short-boosted mice and ≥95 days post 3° from long-boosted mice, enriched for CD8 T cells and sorted for K^b-SIINFEKL-specific CD8 T cells. Either 2×10^3 or 2×10^5 K^b-SIINFEKL-specific CD8 T cells were transferred to CD45.1 mice. One day after transfer, recipients were infected with VSV-OVA and donor CD45.2 K^b-SIINFEKL-specific CD8 T cells from short-boosted (solid line) and long-boosted (dotted line) mice were measured in the blood at the indicated timepoints. Gray lines are low cell number transfers and black lines are high cell number transfers. At all timepoints, there is no significant difference in tetramer+ % between short- and long-boosted cells at low or high numbers of transferred cells. (E) Recipient mice from (D) were sacrificed at day 22 post infection and donor K^b-SIINFEKL-specific CD8 T cells from short-boosted (black) and long-boosted (white) mice were enumerated from spleen. Data in (D) and (E) are representative of 1 experiment N=at least 4.

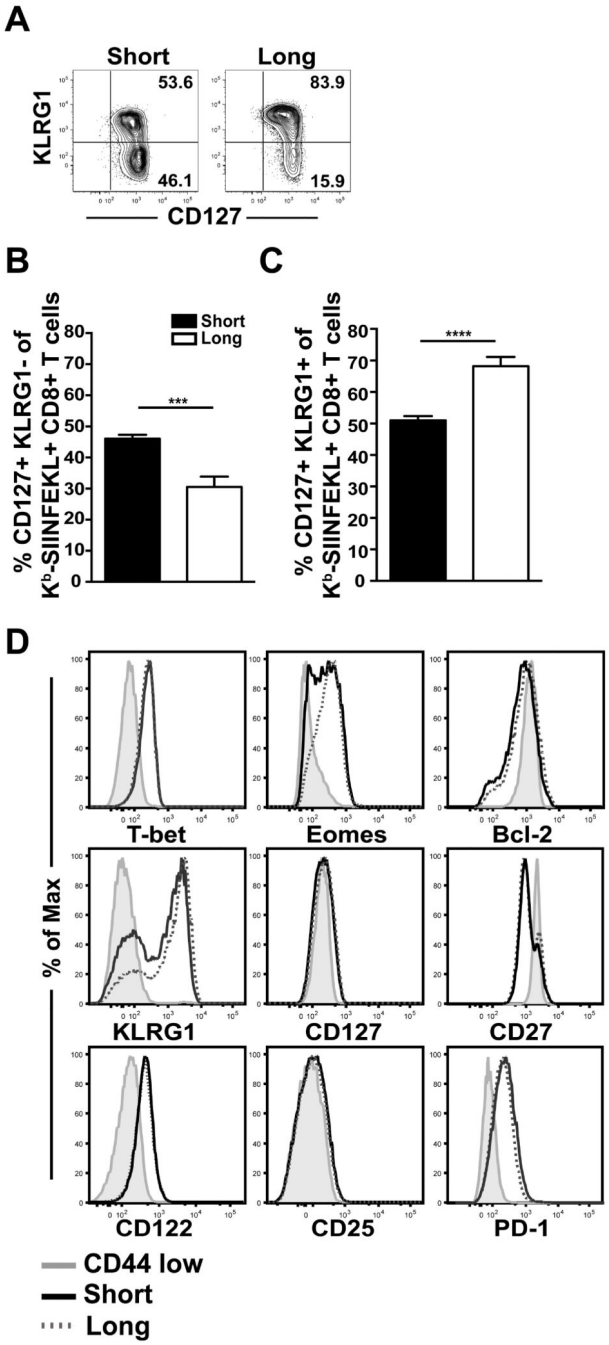

FIGURE 5. Short-boosted Ag-specific CD8 T cells have a memory phenotype

(A) Visualization and (B-C) quantification of KLRG1 and CD127 expression on CD44+ K^b-SIINFEKL tetramer+ CD8 T cells from short-boosted (black) or long-boosted (white) mice at day 30 post 3° immunization. Plots are gated on CD44+ K^b-SIINFEKL tetramer+ CD8 T cells from splenocytes. (D) Expression of indicated proteins on CD44+ K^b-SIINFEKL tetramer+ CD8 T cells from short-boosted (black, solid line) and long-boosted (dotted, grey line) mice; grey filled histograms indicate expression on CD44 low CD8+ T cells. Data are

representative of at least 2 experiments, N=2-5 mice per experiment. Graphs show mean +/− SEM. ***p=0.0001, and **** p <0.0001.

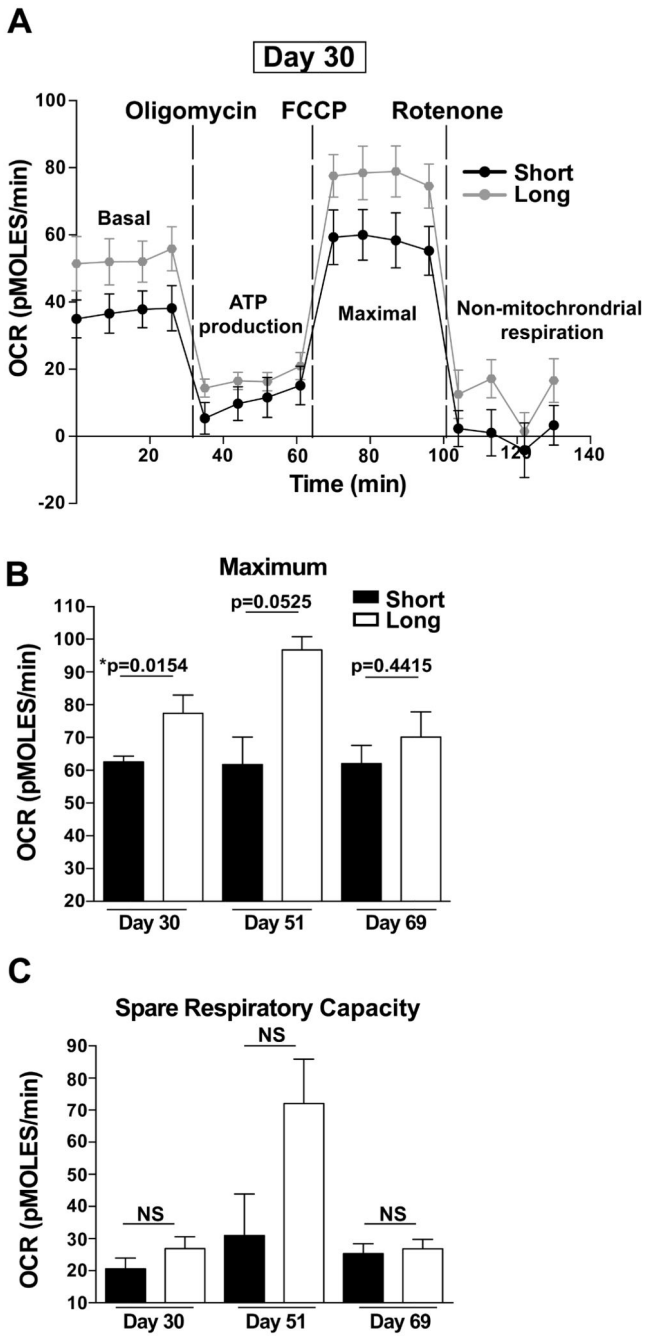

FIGURE 6. Short-boosted Ag-specific CD8 T cells exhibit altered metabolic function

CD44+ K^b-SIINFEKL-specific CD8 T cells were purified at day 30, day 51 and day 69 after 3° short or long HPBB via flow sorting. Oxygen consumption rate (OCR) was measured under basal conditions and after the addition of the indicated mitochondrial inhibitors. Oligomycin is an inhibitor of ATP-synthase and measures ATP-linked respiration; FCCP uncouples electron transport and allows for measuring maximal OCR. Rotenone addition permits measuring non-mitochondrial respiration. (A) Shows raw data from Seahorse platform at day 30 and represents the effects of mitochondrial inhibitors on OCR of short-

boosted (black line) and long-boosted (grey line) of K^b-SIINFEKL-specific CD8 T cells. Raw data from day 51 and day 69 are not shown. (B) Corrected maximal OCR and (C) spare respiratory capacity (SRC) for short-boosted (black) and long-boosted (white) K^b-SIINFEKL-specific CD8 T cells at the indicated timepoints. Data for day 30 are representative of 2 experiments, N=2-6 mice per experiment. Data for day 51 represent 1 experiment, N=2-3 mice. Data for day 69 represent 1 experiment, N=3 of 2-9 mice pooled for short-boost and N=3 either single or 2 mice pooled for long-boost. Graphs show mean +/− SEM. *p=0.0154. Short- and long-boosted K^b-SIINFEKL-specific CD8 T cell OCR cannot be compared across timepoints because varying cell densities were used on different days.

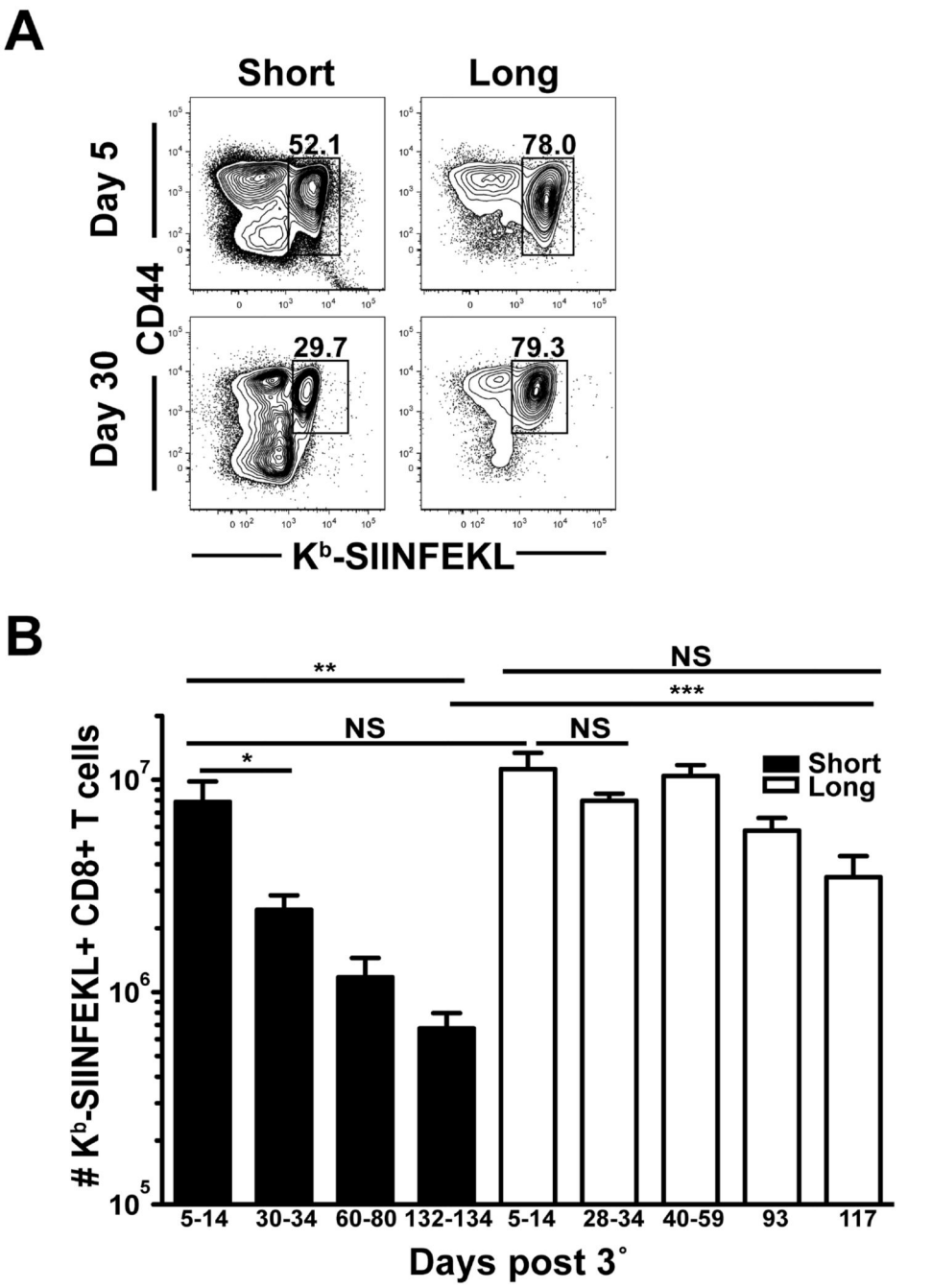

FIGURE 7. Short-boosted Ag-specific CD8 T cells do not form stable memory

Splenocytes were isolated at indicated times after 3° from short-boosted and long-boosted mice. (A) Plots are gated on CD8+ T cells. (B) CD44+ K^b-SIINFEKL+ CD8 T cell numbers were enumerated in short-boosted (black) and long-boosted (white) mice at indicated timepoints. Data are representative of at least 2 experiments, N=2-10 mice per experiment, except day 117 where N=3. Graphs show mean +/− SEM. *p= 0.0174, **p= 0.0023, and *** p = 0.0001.